Disturbance observer and tube-based model reference adaptive control for active suspension systems with non-ideal actuators

Mousavi , Yashar; Zarei, Amin; Kucukdemiral, ibrahim Beklan; Fekih, Afef; Alfi, Alireza

Published in:
Proceedings of the 22nd IFAC World Congress

DOI:
10.1016/j.ifacol.2023.10.1707

Publication date:
2023

Document Version
Publisher's PDF, also known as Version of record

Available online at www.sciencedirect.com

ScienceDirect

IFAC PapersOnline CONFERENCE PAPER ARCHIVE

IFAC PapersOnLine 56-2 (2023) 1075–1081

Disturbance Observer and Tube-based Model Reference Adaptive Control for Active Suspension Systems with Non-ideal Actuators

[1]Yashar Mousavi, [2]Amin Zarei, [1]Ibrahim Beklan Kucukdemiral, [3*]Afef Fekih, [4]Alireza Alfi

[1]*Department of Applied Science, School of Computing, Engineering and Built Environment, Glasgow Caledonian University, Glasgow G4 0BA, UK (e-mail: seyedyashar.mousavi@gcu.ac.uk; ibrahim.kucukdemiral@gcu.ac.uk)*

[2]*Department of Electrical and Computer Engineering, University of Sistan and Baluchestan, Zahedan, Iran (e-mail: amin.zarei@pgs.usb.ac.ir)*

[3]*Electrical and Computer Engineering Department, University of Louisiana at Lafayette, P.O. Box 43890, Lafayette, LA 70504, USA (e-mail: afef.fekih@louisiana.edu)*

[4]*Faculty of Electrical Engineering, Shahrood University of Technology, Shahrood 36199-95161, Iran (e-mail: a_alfi@shahroodut.ac.ir)*

Abstract: Active suspension systems undertake a vital role in ensuring passengers' ride comfort and vehicle vibration attenuation. This work proposes a tube-based model reference adaptive control (TMRAC) that identifies a correctional control component at each time instant for performance amplification of active suspension systems with non-ideal actuators. The TMRAC is augmented by a disturbance observer (DO) to compensate for the effects of dead-zone and hysteresis. Closed-loop stability analysis of the developed method is also investigated in the sense of Lyapunov theory. The developed control scheme's feasibility with regard to suspension safety, road handling, and ride comfort is assessed through simulations by using a class C road profile. Comparison results with DO-based conventional MRAC are also conducted. The obtained results demonstrate that the proposed DO-based control strategy provides a superior ride comfort quality and better road disturbance mitigation with less control effort than the conventional method.

Keywords: Tube-based model reference adaptive control, Disturbance observer, Active suspension system, Vibration, Non-ideal actuator.

1. INTRODUCTION

With the recent advancements in industrial automation, enhancing the performance of vehicle suspension systems has been an ongoing concern in industry and academia. Vehicle suspension systems have always played a critical role in providing satisfactory ride comfort and guaranteeing the vehicle's maneuverability and stability by absorbing the vibrations of road surface Ho et al. (2021). In this context, active suspension systems have been the topic of many research studies due to their characteristics, such as equipping the system with controlled actuators placed between the sprung and unsprung masses to help the active suspensions produce active control force to impede the road-surface-arisen vibrations; and capability to add and dissipate energy when necessary. Benefitting from these features, the active suspension system can provide simultaneous road-handling and ride comfort performance Moradi and Fekih (2014).

During recent decade, numerous research has focused on developing control methodologies for active suspension systems. To attain the desired road handling and passenger comfort performances, adaptive control strategies Mousavi et al. (2022a); Pang et al. (2019), model predictive control Theunissen et al. (2019), and sliding mode control strategies Moradi and Fekih (2013) have been extensively investigated. Although the abovementioned methods' control performance were reported effective, they have failed to make a desirable trade-off between passenger ride comfort and good road holding capability. Accordingly, developing effective control strategies capable of simultaneous guaranteeing ride comfort, road holding, and suspension safety is still a challenging issue that needs to be investigated. Moreover, most literature studies have considered an ideal actuator, while non-ideal actuators in practice suffer from dead-zone and hysteresis, which can negatively affect the suspension system's performance. However, since disturbance observers (DO) have been useful tools to estimate the uncertainties and enhance the controllers' performance

10.1016/j.ifacol.2023.10.1707

Zarei et al. (2019); Mousavi et al. (2022b, 2021); Zarei et al. (2018), incorporating DOs with control strategies can be a solution for dealing with dead-zone and hysteresis effects in suspension systems.

Model reference adaptive control (MRAC) offers an efficient design scheme by an explicit reference system to be followed. Taking advantage of a well-established mathematical proof of stability, MRAC methods compare the system's output with a stabilized reference model and regulate the controller's parameters to stabilize the feedback control system's dynamics. In line with MRAC's desirable performance, many works have employed this technique to deal with practical systems Nguyen et al. (2018); Asiain and Garrido (2021) as well as performance enhancements on MRAC approach Anderson and Marshall (2021); Arab and Mousavi (2020). For instance, in Nguyen et al. (2018), speed tracking control of a surface-mounted motor drive with uncertain parameters was investigated through the MRAC method. Authors in Asiain and Garrido (2021) dealt with disturbances and parametric uncertainties in a servo system by employing a nonlinear MRAC. In another study Ghabraei et al. (2021), an active MRAC-based control approach was developed for vibration suppression of wind turbine blades. A modified MRAC-based control paradigm for nonlinear dynamical systems was proposed in Anderson and Marshall (2021). Aiming at enhancing the conventional MRAC's closed loop tracking performance, a tube-based MRAC approach was proposed in Mirkin and Gutman (2013). The TMRAC divided the control input into adaptive and correction components. The system was augmented by an online optimization technique aiming at finding the correlation between user-defined limits in an on-line manner.

The on-line adaption of the correction control component, which can be defined within user-defined limits, has been found a significant enhancement to conventional MRAC. In this regard, if the results are not satisfactory, the designer can repetitiously modify the limits to achieve the desired specifications. Accordingly, the added flexibility to the controller design has made the tube-based strategy an effective approach in diminishing the control effort, which makes the controller a desirable method for dealing with practical applications. However, despite the method's performance verification on SISO unstable systems Mirkin et al. (2012, 2013), a more thorough evaluation of intricate systems would be needed to validate its performance. Accordingly, this work extends the design process along with the Lyapunov-based stability analysis for the active suspension system with dead-zone and hysteresis nonlinearities in the actuator. Furthermore, since a non-ideal actuator is considered in this study, a disturbance observer is augmented with the developed control scheme to estimate the uncertainties in the actuator. Moreover, simultaneous suspension safety, road handling, and ride comfort requirements are investigated, considering a random road profile simulating the rugged situation. This work contributes the literature as follows:

- An efficient tube-based MRAC approach for MIMO active suspension systems with non-ideal actuators.
- A disturbance observer-based design that ensures the suspension safety and ride comfort while simultaneously mitigates the hysteresis and dead-zone effects resulting from non-ideal actuators.
- A comparative analysis with a DO-based conventional MRAC approach.

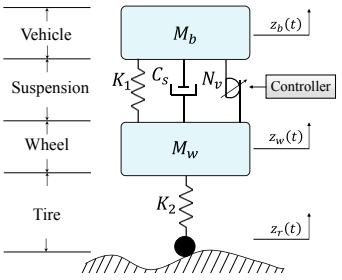

Fig. 1. The quarter-car suspension system.

The remainder of this paper is organized as follows. The problem statement, comprising the system modeling and the performance measures is presented in Section 2. The developed tube-based adaptive control along with the corresponding stability analysis are investigated in Section 3. Section 4 demonstrates the comparative performance validations and simulation results, while Section 5 concludes the paper.

2. PROBLEM STATEMENT

2.1 Quarter-car Active Suspension System

The quarter-car active suspension system (Fig. 1) acts as a bridge between the unsprung and the sprung masses. Considering the vehicle's body and the wheels vertical displacement as the state variables and taking advantage of Lagrange's modeling, the state-space representation of motion can be expressed as Mousavi et al. (2022a):

$$\mathcal{M}_b \ddot{z}_b = \mathcal{N}_v - \mathcal{C}_s\left(\dot{z}_b - \dot{z}_w\right) - \mathcal{K}_1\left(z_b - z_w\right), \tag{1a}$$

$$\mathcal{M}_w \ddot{z}_w = -\mathcal{N}_v + \mathcal{C}_s\left(\dot{z}_b - \dot{z}_w\right) + \mathcal{K}_1\left(z_b - z_w\right) - \mathcal{K}_2\left(z_w - z_r\right), \tag{1b}$$

where the sprung mass $\mathcal{M}_b$ stands for the quarter vehicle's body mass, and the unsprung mass $\mathcal{M}_w$ represents the combined wheel and axle mass. A linear spring with stiffness $\mathcal{K}_2$ models the tire, and the passive parts of the system comprise a linear damper with damping coefficient $\mathcal{C}_s$ and a linear spring with stiffness $\mathcal{K}_1$. $\mathcal{N}_v$ denotes the hydraulic actuation force which will be defined later on. $z_r(t)$ represents the vertical road profile, and the unsprung and sprung masses' vertical displacements are $z_w(t)$ and $z_b(t)$, respectively. Any change in the payloads results in changes in the vehicle mass $\mathcal{M}_b$, and also, gradual changes of stiffness and damping coefficients over time is possible. Hence, a priori knowledge of the model is needed to fulfill a functional control performance.

Assumption 1. During horizontal motion, we assume the vehicle's speed remains constant. In this sense, the vertical movements of the vehicle can be interpreted as white noise, an acceptable approximation for the actual situation.

Assumption 2. Measurement information is assumed to be available for all state variables.

Defining $\Delta = [z_b - z_w \;\; z_w - z_r \;\; \dot{z}_b \;\; \dot{z}_w]^T = [\delta_1 \;\; \delta_2 \;\; \delta_3 \;\; \delta_4]^T$, with δ_1, δ_2, δ_3, and δ_4 being the body and wheel dis-

placements, and absolute vertical speeds, respectively. The dynamic equation (1) can be rewritten in as

$$\dot{\Delta}(t) = \mathcal{A}\Delta(t) + \mathcal{B}\upsilon(t), \tag{2}$$

where $\upsilon(t)$ is the control input, and

$$\mathcal{A} = \begin{bmatrix} 0 & 0 & 1 & -1 \\ 0 & 0 & 0 & 1 \\ -\frac{\mathcal{K}_1}{\mathcal{M}_b} & 0 & -\frac{\mathcal{C}_s}{\mathcal{M}_b} & \frac{\mathcal{C}_s}{\mathcal{M}_b} \\ \frac{\mathcal{K}_1}{\mathcal{M}_w} & -\frac{\mathcal{K}_2}{\mathcal{M}_w} & \frac{\mathcal{C}_s}{\mathcal{M}_w} & -\frac{\mathcal{C}_s}{\mathcal{M}_w} \end{bmatrix}, \ \mathcal{B} = \begin{bmatrix} 0 & 0 \\ 0 & -1 \\ \frac{1}{\mathcal{M}_b} & 0 \\ -\frac{1}{\mathcal{M}_w} & 0 \end{bmatrix}. \tag{3}$$

2.2 Non-ideal Actuator

In this paper, the non-ideal actuator $\mathcal{N}_\upsilon$ is assumed to be affected by hysteresis and dead-zone. The output of non-ideal actuator can be modeled by a nonlinear hysteresis as Pan et al. (2017).

$$\mathcal{N}_{\upsilon,hys} = \eta\kappa\upsilon + (1-\eta)\kappa\omega_h = \eta_1\upsilon + \eta_2\omega_h, \tag{4}$$

where the pseudo-natural frequency of the nonlinearity is referred as κ, $0 < \eta < 1$ is the stiffness ratio, υ is the input to the actuator, η_1 and η_2 are positive parameters, and the auxiliary variable ω_h is defined as follows:

$$\dot{\omega}_h = \dot{\upsilon} - \xi|\dot{\upsilon}|\,|\omega_h|^{n-1}\omega_h - \rho\dot{\upsilon}|\omega_h|^n, \ \omega_h(0) = 0, \tag{5}$$

with $\xi > 0$, $\rho > 0$, and $n > 0$ controlling the magnitude and shape of the hysteresis loop so that $\xi > |\rho|$ and $n \geq 1$.

When the non-ideal actuator is modeled by dead-zone, it has the form of $\mathcal{N}_{\upsilon,dz} = \alpha\upsilon + W$, Tao and Kokotovic (1996), where

$$W = \begin{cases} -\alpha b_l, & \upsilon \leq b_l \\ -\alpha\upsilon, & b_l < \upsilon < b_r \\ -\alpha b_r, & \upsilon \geq b_r \end{cases} \tag{6}$$

where $b_r > 0$ and $b_l > 0$ are unknown bounds and α is the pseudo slope of the dead-zone characteristics.

Since the coefficients of aforementioned equations are unknown, a unified actuator output is employed as follows:

$$\mathcal{N}_\upsilon = H\upsilon + D(t), \tag{7}$$

where H can be considered as $H = \eta_1$ and $H = \alpha$ for hysteresis and dead-zone cases, respectively. $D(t)$ is a disturbance term constructed by nonlinear hysteresis or dead-zone to be estimated by the DO. It is noteworthy that, when both hysteresis and dead-zone are present model, definition (7) remains unchanged. Hence, $\mathcal{N}_\upsilon = \mathcal{N}_{\upsilon,hys} + \mathcal{N}_{\upsilon,dz}$ is considered in this work.

2.3 Performance Measures

As performance requirements for the suspension system, the ride comfort, wheel-road handling, and suspension safety are supposed to be met. To provide a preferable riding comfort, the system should absorb the vibrations and effectively isolate the vehicle's body and passengers from road fluctuations, that implies respecting the suspension deflection within its permissible limit $|z_b - z_w| \leq z_{\max}$. In addition, maintaining a continuous road-wheel contact is essential to ensure vehicle handling and safe riding. Defining the dynamic tire force as

$$f_{tire,dyn} = \begin{cases} 0, & \text{if } \mathcal{K}_2(z_w - z_r) \geq f_{tire,st} \\ \mathcal{K}_2(z_w - z_r), & \text{if } \mathcal{K}_2(z_w - z_r) < f_{tire,st} \end{cases} \tag{8}$$

with g and $f_{tire,st} = g(\mathcal{M}_b + \mathcal{M}_w)$ being the gravitational constant and static tire force, respectively, the relative tire force $RTF = f_{tire,dyn}/f_{tire,st}$ is the ratio of dynamic to static forces. It is noteworthy that, keeping the magnitude of $RTF < 1$ guarantees the road handling. Moreover, the rattle space limit, which is the area between the $\mathcal{M}_b$ and $\mathcal{M}_w$ when the vehicle is at rest position stationary, is considered as a suspension safety measure. Accordingly, the relative suspension deflection is

$$RSD = \frac{z_b(t) - z_w(t)}{z_r(t)}. \tag{9}$$

It is worth mentioning that to guarantee that the rattle space limit remains unviolated, the magnitude of RSD must be $RSD < 1$. Accordingly, this paper aims to ensure the satisfactory ride comfort performance and ensure the essential suspension requirements to improve the vehicle handling quality.

3. TUBE-BASED ADAPTIVE CONTROL

This section describes the proposed controller's design procedure. The closed-loop stability analysis is investigated in detail, and then the controller is designed for the problem at hand.

3.1 Disturbance Observer Design

According to (1) and (7), the following equation with lumped uncertainty $D_l(t)$ is resulted as follows:

$$\dot{\delta}_3 = \frac{1}{\mathcal{M}_{bn}}\Big(-\mathcal{K}_{1n}\delta_1 - \mathcal{C}_{sn}(\delta_3 - \delta_4) + H_n\upsilon\Big) + D_l(t) \tag{10}$$

where $\mathcal{M}_{bn}$, $\mathcal{K}_{ln}$, $\mathcal{C}_{sn}$, and H_n are known nominal values of $\mathcal{M}_b$, $\mathcal{K}_l$, $\mathcal{C}_s$, and H, respectively. $D_l(t)$ encompasses the uncertainties in the suspension parameters and sprung mass as well as actuator imperfections. It can be expressed as:

$$D_l(t) = \frac{1}{\mathcal{M}_b}\Big(-\mathcal{K}_1\delta_1 - \mathcal{C}_s(\delta_3 - \delta_4) + H\upsilon + D(t)\Big) \tag{11}$$

The lumped uncertainty $D_l(t)$ must be tackled in the closed-loop system mechanism using the control input. In this paper, the following DO is proposed to estimate lumped uncertainty $D_l(t)$:

$$\hat{D}_l(t) = \theta(t) + \lambda\delta_3 + \int_0^t \hat{D}_l(\tau)\,d\tau, \tag{12a}$$

$$\dot{\theta}(t) = -(\lambda+1)\hat{D}_l(t) - \frac{\lambda}{\mathcal{M}_{bn}}\Big(-\mathcal{K}_{1n}\delta_1 - \mathcal{C}_{sn}(\delta_3 - \delta_4) + H_n\upsilon\Big), \tag{12b}$$

where $\theta(t)$ is the internal state variable, $\hat{D}_l(t)$ is the estimation of $D_l(t)$, and λ is the observer gain. Defining the disturbance estimation error as $\tilde{D}_l(t) = \hat{D}_l(t) - D_l(t)$, based on (10) and (12), the derivation of $\tilde{D}_l(t)$ yields

$$\dot{\tilde{D}}_l(t) = -\dot{D}_l(t) - \lambda\tilde{D}_l(t). \tag{13}$$

Remark 1. It is noteworthy that when $D_l(t)$ is almost constant or $\dot{D}_l(t) \cong 0$, $\lim_{t\to\infty}\dot{\tilde{D}}_l(t) \cong 0$ for $\lambda > 0$.

3.2 Proposed Controller Design

Let us assume that some of the reference system's parameters can vary within an admissible range. The developed method replaces the classic adaptive objective with a predestined optimal trajectory with a tube-based reference model. Defining υ_c as a correction control signal being applied to the reference system and by setting its constraints, using the performance tube one can generate a set of preferable paths that fits the closed-loop system's characteristics. Accordingly, two purposes can be identified: a) the output and states of the main system will closely follow their respective references, and b) ensuring admissible ranges for υ_c so as to meet additional criteria. In light of the fact that both purposes are independent, the TMRAC design can be carried out in two steps. First, to ensure the closed-loop system's stability and asymptotic tracking of the optimal paths, the control input should be defined. Then, a mechanism for adjusting υ_c should be investigated to attain more performance requirements, including control effort or the control signal's domain constraints. Hence, an additional functional characteristic as a square function of the control signal is considered.

Let us consider system (2) in the state-space, with $\mathcal{A} \in \mathbb{R}^{n\times n}$ and $\mathcal{B} \in \mathbb{R}^{n\times m}$ being unknown constant matrices, and the system's input and state variable vectors be $\upsilon \in \mathbb{R}^{m\times 1}$ and $\Delta \in \mathbb{R}^{n\times 1}$, respectively. The primary purpose is to construct the TMRAC in such a way that the system follows the reference system below.

$$\dot{\Delta}_r = \mathcal{A}_r\Delta_r + \mathcal{B}_r\upsilon_r, \tag{14a}$$
$$\upsilon_r(t) = \upsilon_c(t) + r(t), \tag{14b}$$

where $r(t)$ and $\Delta_r \in \mathbb{R}^{n\times 1}$ denote the standard reference input and the reference state variables,respectively, the stable matrix $A_r \in \mathbb{R}^{n\times n}$ and $B_r \in \mathbb{R}^{n\times m}$ are known constant matrices, and the reference input vector $\upsilon_r \in \mathbb{R}^{m\times 1}$ with the control objective correction vary within specified given limits $\upsilon_c(t) \in \left[\upsilon_c^-\ \upsilon_c^+\right]$, with υ_c^- and υ_c^+ being the lower and upper limits, respectively. The control input $\upsilon(t)$ can be shown as

$$\upsilon(t) = \upsilon_a(t) + \upsilon_c(t) - \hat{D}_l(t). \tag{15}$$

where $\upsilon_a(t)$ is an adaptive term.

Accordingly, $\upsilon_c(t)$ can determine the function affiliated with the system. An optimization problem can be formulated for controller design:

$$\begin{aligned} &Minimize\ J\ (\upsilon_c) = \upsilon^2(t) \\ &s.t: \upsilon_c^- < \upsilon_c(t) \le \upsilon_c^+ \end{aligned} \tag{16}$$

Specifying the error as $e(t) = \Delta(t) - \Delta_r(t)$ yields the following error dynamics

$$\dot{e}(t) = \mathcal{A}\Delta(t) + \mathcal{B}\upsilon(t) - \mathcal{A}_r\Delta_r(t) - \mathcal{B}_r\upsilon_r(t). \tag{17}$$

Assumption 3. In accordance with the compatibility conditions, assume the existence of a vector gain $\Gamma^* = [\Gamma_1^*, \Gamma_2^*]$, $\Gamma_1^* \in \mathbb{R}^{n\times m}$ and $\Gamma_2^* \in \mathbb{R}^{m\times m}$ such that $\mathcal{A}_r = \mathcal{A} + \mathcal{B}\Gamma_1^{*T}$ and $\mathcal{B}_r = \mathcal{B}\Gamma_2^*$.

Accordingly, rewriting (17) yields

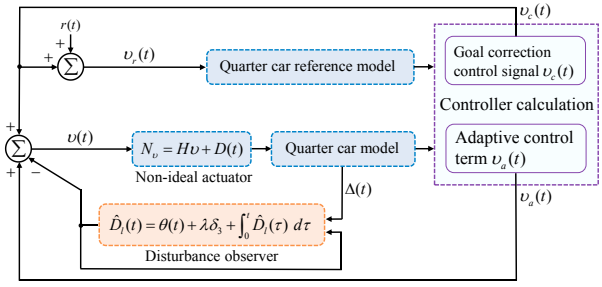

Fig. 2. The proposed DO-based TMRAC.

$$\begin{aligned} \dot{e}(t) &= \left(\mathcal{A}_r - \mathcal{B}\Gamma_1^{*T}\right)\Delta(t) + \mathcal{B}\upsilon(t) - \mathcal{A}_r\Delta_r(t) - \mathcal{B}_r\upsilon_r(t) \\ &= \mathcal{A}_r e(t) - \mathcal{B}\Gamma_1^{*T}\Delta(t) \\ &+ \mathcal{B}\left(-\hat{D}_l(t) + \upsilon_a(t) - \Gamma_2^* r(t) - \Gamma_c^*\upsilon_c,(t)\right), \end{aligned} \tag{18}$$

with $\Gamma_c^* = \Gamma_2^* - I$ and I representing the identity matrix, and $\upsilon_a(t)$ is

$$\upsilon_a(t) = \Gamma_1^T\Delta(t) + \Gamma_2 r(t) + \Gamma_c\upsilon_c(t), \tag{19}$$

where Γ_1^* and Γ_2^* are approximated by $\Gamma_1 \in \mathbb{R}^{n\times m}$ and $\Gamma_2 \in \mathbb{R}^{m\times m}$, respectively. Substituting (19) into (18) yields

$$\begin{aligned} \dot{e}(t) &= \mathcal{A}_r e(t) - \mathcal{B}\Gamma_1^{*T}\Delta(t) - \mathcal{B}\hat{D}_l(t) + \mathcal{B}\Gamma_1^T\Delta(t) \\ &+ \mathcal{B}\Gamma_2 r(t) + \mathcal{B}\Gamma_c\upsilon_c(t) - \mathcal{B}\Gamma_2^* r(t) - \mathcal{B}\Gamma_c^*\upsilon_c(t) \\ &= \mathcal{A}_r e(t) - \mathcal{B}\hat{D}_l(t) + \mathcal{B}\left(\Gamma_1^T - \Gamma_1^{*T}\right)\Delta(t) \\ &+ \mathcal{B}\left(\Gamma_2 - \Gamma_2^*\right) r(t) + \mathcal{B}\left(\Gamma_c - \Gamma_c^*\right)\upsilon_c(t). \end{aligned} \tag{20}$$

The control objective is reached by determining appropriate adaptive laws to update the vector gains and the observer gain; i.e. $e(t) \to 0$ and $\tilde{D}_l(t) \to 0$ as $t \to \infty$. With the parametric errors defined as $\tilde{\Gamma}_1 = \Gamma_1 - \Gamma_1^*$, $\tilde{\Gamma}_2 = \Gamma_2 - \Gamma_2^*$, and $\tilde{\Gamma}_c = \Gamma_c - \Gamma_c^*$ one obtains

$$\dot{e}(t) = \mathcal{A}_r e(t) - \mathcal{B}\hat{D}_l(t) + \mathcal{B}\tilde{\Gamma}_1^T\Delta(t) + \mathcal{B}\tilde{\Gamma}_2 r(t) + \mathcal{B}\tilde{\Gamma}_c\upsilon_c(t) \tag{21}$$

Figure 2 illustrates the control scheme's block diagram.

.

Remark 2. Γ_1^* and Γ_2^* are constant values, while Γ_1 and Γ_2 are time-dependant. Nonetheless, for simplicity of writing the time t index is omitted.

3.3 Stability Analysis

Considering $P \in \mathbb{R}^{n\times n}$ a positive definite symmetric matrix, and neglecting the time index "t" for simplification of writing, the Lyapunov function candidate is expressed as

$$\begin{aligned} V(t) &= e^T Pe + \frac{1}{2}\tilde{D}_l^2 + \frac{1}{2}tr\left[\tilde{\Gamma}_1^T M^{-1}\tilde{\Gamma}_1\right] \\ &+ \frac{1}{2}tr\left[\tilde{\Gamma}_2^T M^{-1}\tilde{\Gamma}_2\right]\frac{1}{2}tr\left[\tilde{\Gamma}_c^T M^{-1}\tilde{\Gamma}_c\right], \end{aligned} \tag{22}$$

with $tr[\cdot]$ representing the trace of the matrix.

A positive definite matrix $Q \in \mathbb{R}^{m\times m}$ can be defined such that $M = \Gamma^* Q = (\Gamma^* Q)^T = Q^T\Gamma^{*T} > 0$. The time derivation of (23) yields

$$\begin{aligned} \dot{V}(t) &= \dot{e}^T Pe + e^T P\dot{e} + \dot{\tilde{D}}_l\tilde{D}_l + tr\left[\dot{\tilde{\Gamma}}_1^T M^{-1}\tilde{\Gamma}_1\right] \\ &+ tr\left[\dot{\tilde{\Gamma}}_2^T M^{-1}\tilde{\Gamma}_2\right] + tr\left[\dot{\tilde{\Gamma}}_c^T M^{-1}\tilde{\Gamma}_c\right]. \end{aligned} \tag{23}$$

Using (13) and by substituting (21) into (24), we have

$$\dot{V}(t) = \left[e^T \mathcal{A}_r^T + \Delta^T \tilde{\Gamma}_1 \mathcal{B}^T + r^T \tilde{\Gamma}_2^T \mathcal{B}^T + \upsilon_c^T \tilde{\Gamma}_c^T \mathcal{B}^T\right] Pe \tag{24}$$
$$+ e^T P \left[\mathcal{A}_r e + \mathcal{B}\tilde{\Gamma}_1^T \Delta + \mathcal{B}\tilde{\Gamma}_2 r + \mathcal{B}\tilde{\Gamma}_c \upsilon_c\right]$$
$$- \dot{D}_l \tilde{D}_l - \lambda \tilde{D}_l^2 + tr\left[\dot{\tilde{\Gamma}}_1^T M^{-1} \tilde{\Gamma}_1\right]$$
$$+ tr\left[\dot{\tilde{\Gamma}}_2^T M^{-1} \tilde{\Gamma}_2\right] + tr\left[\dot{\tilde{\Gamma}}_c^T M^{-1} \tilde{\Gamma}_c\right].$$

Lemma 3. Cao et al. (1998), Assuming X and Y real matrices with appropriate dimensions, the inequality $X^T Y + Y^T X \leq \beta X^T X + \beta^{-1} Y^T Y$ always holds for any scalar $\beta > 0$.

Lemma 4. Freeman and Kokotovic (2008), Assuming the existence of a continuous positive definite Lyapunov function $V(\Phi) \geq 0$ (with bounded initial conditions) satisfying $\sigma_1(\|\phi\|) \leq V(\phi, t) \leq \sigma_2(\|\phi\|)$ such that $\dot{V}(\Phi) \leq -c_1 V(\Phi) + c_2$, with $\sigma_1, \sigma_2 : \mathbb{R}^n \to \mathbb{R}$ being class $\mathcal{K}$ functions, and $c_1 > 0$ and $c_2 > 1$, the uniformly roundedness of the solution is ensured.

Having Lemma 3 with $\beta = 1$, (25) can be rewritten as

$$\dot{V}(t) \leq e^T \left(\mathcal{A}_r^T P + P\mathcal{A}_r\right) e + 2e^T P \mathcal{B}\tilde{\Gamma}_1 \Delta(t) \tag{25}$$
$$+ 2e^T P \mathcal{B}\tilde{\Gamma}_2 r + 2e^T P \mathcal{B}\tilde{\Gamma}_c \upsilon_c$$
$$- \frac{1}{2}\dot{D}_l^2 - \frac{1}{2}\tilde{D}_l^2 - \lambda \hat{D}_l^2 + tr\left[\dot{\tilde{\Gamma}}_1^T M^{-1} \tilde{\Gamma}_1\right]$$
$$+ tr\left[\dot{\tilde{\Gamma}}_2^T M^{-1} \tilde{\Gamma}_2\right] + tr\left[\dot{\tilde{\Gamma}}_c^T M^{-1} \tilde{\Gamma}_c\right].$$

Choosing P that satisfies $\mathcal{A}_r^T P + P\mathcal{A}_r = -L$, where L is a positive definite matrix, yields

$$\dot{V}(t) \leq -e^T L e + 2e^T P \mathcal{B}\tilde{\Gamma}_1 \Delta \tag{26}$$
$$+ 2e^T P \mathcal{B}\tilde{\Gamma}_2 r + 2e^T P \mathcal{B}\tilde{\Gamma}_c \upsilon_c$$
$$+ \frac{1}{2}\|\dot{D}_l\|^2 - (\lambda + \frac{1}{2})\tilde{D}_l^2 + tr\left[\dot{\tilde{\Gamma}}_1^T M^{-1} \tilde{\Gamma}_1\right]$$
$$+ tr\left[\dot{\tilde{\Gamma}}_2^T M^{-1} \tilde{\Gamma}_2\right] + tr\left[\dot{\tilde{\Gamma}}_c^T M^{-1} \tilde{\Gamma}_c\right].$$

where $\|\dot{D}_l\| \leq \rho_d$, $\rho_d > 0$, and $\lambda > 0$. Having the positive definite L, $-e^T L e$ is always negative definite. Consequently, to realize the closed-loop stability $\dot{V}(t) \leq 0$, the following relationships must be established.

$$tr\left[\dot{\tilde{\Gamma}}_1^T M^{-1} \tilde{\Gamma}_1\right] = -2e^T P \mathcal{B}\tilde{\Gamma}_1 \Delta, \tag{27a}$$
$$tr\left[\dot{\tilde{\Gamma}}_2^T M^{-1} \tilde{\Gamma}_2\right] = -2e^T P \mathcal{B}\tilde{\Gamma}_2 r, \tag{27b}$$
$$tr\left[\dot{\tilde{\Gamma}}_c^T M^{-1} \tilde{\Gamma}_c\right] = -2e^T P \mathcal{B}\tilde{\Gamma}_c \upsilon_c. \tag{27c}$$

Considering the above-mentioned compatibility conditions, the following regulation rules can be derived.

$$\dot{\tilde{\Gamma}}_1 = -2Q^T \mathcal{B}_r P e \Delta^T, \tag{28a}$$
$$\dot{\tilde{\Gamma}}_2 = -2Q^T \mathcal{B}_r^T P e r^T, \tag{28b}$$
$$\dot{\tilde{\Gamma}}_c = -2Q^T \mathcal{B}_r^T P e \upsilon_c^T. \tag{28c}$$

Therefore, according to Lemma 4 all closed-loop signals are uniformly bounded.

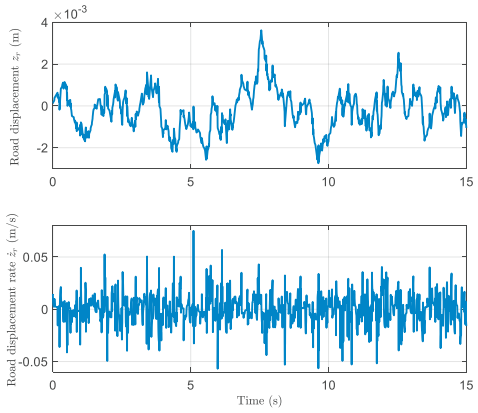

Fig. 3. The class C random road profile.

4. SIMULATION RESULTS AND DISCUSSIONS

The developed control scheme's performance is assessed through simulations for a quarter-car suspension system with dead-zone and hysteresis. The considered quarter-car suspension system and the controller parameters are given in Table 1 in the Appendix section, Lian (2012). The observer gain λ is considered to achieve fast disturbance estimation while maintaining accuracy. The developed controller's performance is assessed in respect of predefined performance measures (Section 2.3) in comparison with conventional MRAC Nguyen (2018) approach. In addition, to maintain fairness in comparative assessments, the proposed DO is used with the conventional MRAC to estimate lumped uncertainty. In order to demonstrate the practical road surface irregularities, as per ISO 8608 ISO/TC et al. (1995), a road profile of class C randomness is considered. The road profile is generated through the first order dynamics as follows:

$$\dot{z}_r = -\delta V z_r + \varpi, \tag{29}$$

where V denotes the vehicle speed and ϖ is a white noise process with spectral density $\Gamma_\varpi = 2\delta V \sigma^2$ (see Tyan et al. (2009) for more details). The vehicle is assumed to run at a constant speed $V = 30$ [m/s], and δ and σ are considered as in Table 1, Tyan et al. (2009).

Remark 5. It should be emphasized that, since the case of a suspension system with a non-ideal actuator is considered in this study, comparing a DO-based control approach with a non-DO-based controller violates the fair comparison. Hence, to validate the performance of the proposed DO and TMRAC, the DO is augmented with the conventional MRAC as well and compared with the TMRAC.

The main function of suspension systems is to attenuate vehicle vibrations and ensure passenger's comfort ride. Therefore, the suspension system's performance directly impacts vertical displacement and ride comfort of the vehicle. Figures 4 and 5 illustrate the closed-loop responses of sprung displacements and speeds, respectively. From Fig. 4, one can see that the wheel displacement is similar for both control techniques; however, the DO-based MRAC's performance is still inferior to that of DO-TMRAC. From Fig. 4, the MRAC appears to have a suboptimal the suspension deflection performance, while in contrast, the developed DO-TMRAC delivers a desirable performance

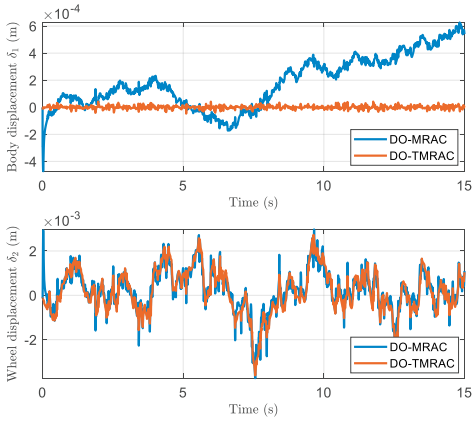

Fig. 4. Body and wheel vertical displacement; a comparison between DO-MRAC and DO-TMRAC approaches.

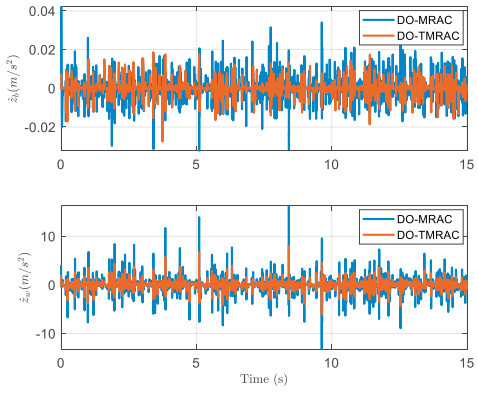

Fig. 5. Body and wheel vertical speed; a comparison between DO-MRAC and DO-TMRAC approaches.

albeit the non-ideal actuator conditions. From Fig. 5, it can be observed that the DO-TMRAC outperforms the DO-MRAC and provides a more mitigated body displacement, and efficaciously suppresses the road surface vibrations, delivering more ride comfort for the passengers.

The comparative *RTF* and *RSD* obtained by the two control approaches under study are depicted in Fig. 6. Note that both control techniques have kept the magnitude of $RTF < 1$ and have guaranteed the road holding. However, with $RTF_{TMRAC} \in (-0.218, 0.165)$, the DO-TMRAC has outperformed the DO-MRAC with $RTF_{MRAC} \in (-0.345, 0.281)$ by keeping the *RTF* in a smaller range. Analogously, both approaches have kept *RSD* within its permissible limit and have guaranteed the suspension safety objective; however, superior performance of the DO-TMRAC is apparent, confirming its efficiency by providing more ride comfort. Furthermore, the actuator force is shown in Fig. 7. It can be seen that the DO-TMRAC has demonstrated a desirable suspension performance with less effort.

Moreover, the extend of improvement in the riding comfort when using the DO-TMRAC is further assessed using the root mean square (RMS) values of the system's outputs. The RMS value for a typical signal $\Delta(t)$ can be calculated as

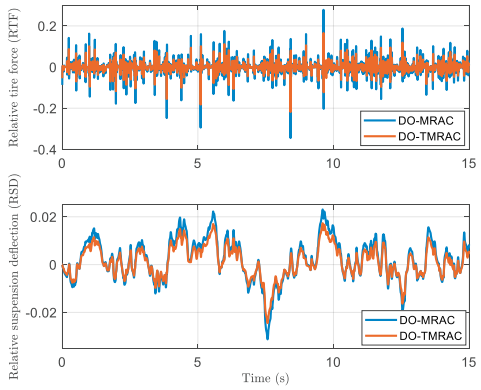

Fig. 6. RTF and RSD for Case 2; a comparison between DO-MRAC and DO-TMRAC approaches.

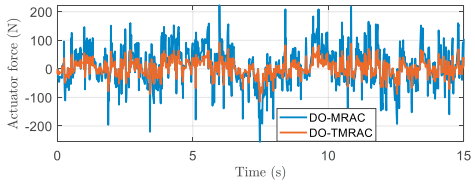

Fig. 7. Actuator force for Case 2; a comparison between DO-MRAC and DO-TMRAC approaches.

$$RMS_{\Delta(t)} = \left(\frac{1}{T} \int_0^T \Delta^2(t)\, dt \right)^{\frac{1}{2}}, \tag{30}$$

where T denotes the simulation time.

The RMS values for the actuator force, and sprung displacement and speed under Class C random road profile are illustrated in Table 2 in the Appendix section. Accordingly, the proposed DO-TMRAC has shown improvements in the ride comfort quality and road disturbance attenuation with less actuator force compared to that of DO-MRAC. The above simulation results confirm the effectiveness of the proposed control scheme in negating the effects of dead-zone and hysteresis. They also confirmed its superior performance compared to DO-MRAC.

5. CONCLUSIONS

This paper developed a disturbance observer tube-based MRAC (DO-TMRAC) scheme for active suspension systems with actuators subject to dead-zone and hysteresis. An ISO class C road profile was used to assess the controller's performance in terms of suspension safety, road handling, and ride comfort. The obtained results confirmed the outstanding performance of the DO-TMRAC in terms of road disturbance mitigation and ride comfort quality improvement.

Additionally, the investigations showed that augmenting the TMRAC with a DO enables the remarkable compensation of non-ideal actuator's effects. Comparative investigations with a DO-based conventional MRAC showed that the proposed DO-TMRAC scheme imposed less control effort to favorably compensate for the effects of dead-zone and hysteresis, and demonstrated remarkable vibration suppression performance. In addition, although both approaches were able to maintain tire forces and suspen-

sion deflection constraints within their permissible ranges, the DO-TMRAC outperformed the DO-MRAC with less magnitudes, guaranteeing better road holding and more suspension safety.

APPENDIX

Table 1. Model and controller parameters.

Parameter	Value	Unit	Parameter	Value	Unit
$\mathcal{M}_b$	250	kg	κ	1.8	
$\mathcal{M}_w$	50	kg	α	1	
$\mathcal{K}_1$	16	kN/m	η_1	1.1	
$\mathcal{K}_2$	160	kN/m	η_2	1	
$\mathcal{C}_s$	1.5	kN s/m	ξ	1.1	
V	30	m/s	ρ	0.5	
δ	16E-6	m^3	n	1	
σ	8E-3	m	b_l	3	
λ	10		b_r	2	

Table 2. RMS values for class C random road profile.

Method	δ_1 (m)	δ_3 (m)	Actuator force (N)
DO-MRAC	6.2312e-04	0.0149	53.5120
DO-TMRAC	2.2779e-05	0.0033	28.3421

REFERENCES

Anderson, R.B. and Marshall, J.A. (2021). Novel model reference adaptive control laws for improved transient dynamics and guaranteed saturation constraints. *Journal of the Franklin Institute*, 358(12), 6281–6308.

Arab, A. and Mousavi, Y. (2020). Optimal control of wheeled mobile robots: From simulation to real world. In *2020 American Control Conference (ACC)*, 583–589. IEEE.

Asiain, E. and Garrido, R. (2021). Anti-chaos control of a servo system using nonlinear model reference adaptive control. *Chaos, Solitons & Fractals*, 143, 110581.

Cao, Y.Y., Sun, Y.X., and Cheng, C. (1998). Delay-dependent robust stabilization of uncertain systems with multiple state delays. *IEEE Trans. on Automatic Control*, 43(11), 1608–1612.

Freeman, R. and Kokotovic, P.V. (2008). *Robust nonlinear control design: state-space and Lyapunov techniques*. Springer Science & Business Media.

Ghabraei, S., Moradi, H., and Vossoughi, G. (2021). Robust adaptive reference model control of nonlinear wind-induced oscillations of floating offshore wind turbine blade in finite-time. *Ocean Engineering*, 241, 110019.

Ho, C.M., Tran, D.T., and Ahn, K.K. (2021). Adaptive sliding mode control based nonlinear disturbance observer for active suspension with pneumatic spring. *Journal of Sound and Vibration*, 116241.

ISO/TC, T.C., Vibration, M., Measurement, S.S.S., of Mechanical Vibration, E., and as Applied to Machines, S. (1995). *Mechanical Vibration–Road Surface Profiles–Reporting of Measured Data*, volume 8608. International Organization for Standardization.

Lian, R.J. (2012). Enhanced adaptive self-organizing fuzzy sliding-mode controller for active suspension systems. *IEEE Trans. on Industrial Electronics*, 60(3), 958–968.

Mirkin, B. and Gutman, P.O. (2013). Tube model reference adaptive control. *Automatica*, 49(4), 1012–1018.

Mirkin, B., Gutman, P.O., and Shtessel, Y. (2012). Tube reference model based direct adaptive control. *IFAC Proceedings Volumes*, 45(13), 553–558.

Mirkin, B., Gutman, P.O., and Shtessel, Y. (2013). Tube-based distributed adaptive control of interconnected linear systems. *IFAC Proceedings Volumes*, 46(27), 55–60.

Moradi, M. and Fekih, A. (2013). Adaptive pid-sliding-mode fault-tolerant control approach for vehicle suspension systems subject to actuator faults. *IEEE Trans. on Vehicular Technology*, 63(3), 1041–1054.

Moradi, M. and Fekih, A. (2014). A stability guaranteed robust fault tolerant control design for vehicle suspension systems subject to actuator faults and disturbances. *IEEE Trans. on Control Systems Technology*, 23(3), 1164–1171.

Mousavi, Y., Alfi, A., Kucukdemiral, I.B., and Fekih, A. (2022a). Tube-based model reference adaptive control for vibration suppression of active suspension systems. *IEEE/CAA Journal of Automatica Sinica*, 9(4), 728–731.

Mousavi, Y., Bevan, G., Kucukdemiral, I.B., and Fekih, A. (2022b). Active fault-tolerant fractional-order terminal sliding mode control for dfig-based wind turbines subjected to sensor faults. In *IEEE IAS Global Conference on Emerging Technologies (GlobConET'22)*. IEEE.

Mousavi, Y., Zarei, A., Mousavi, A., and Biari, M. (2021). Robust optimal higher-order-observer-based dynamic sliding mode control for vtol unmanned aerial vehicles. *International Journal of Automation and Computing*, 18(5), 802–813.

Nguyen, A.T., Rafaq, M.S., Choi, H.H., and Jung, J.W. (2018). A model reference adaptive control based speed controller for a surface-mounted permanent magnet synchronous motor drive. *IEEE Trans. on Industrial Electronics*, 65(12), 9399–9409.

Nguyen, N.T. (2018). Model-reference adaptive control. In *Model-Reference Adaptive Control*. Springer.

Pan, H., Sun, W., Jing, X., Gao, H., and Yao, J. (2017). Adaptive tracking control for active suspension systems with non-ideal actuators. *Journal of Sound and Vibration*, 399, 2–20.

Pang, H., Zhang, X., Chen, J., and Liu, K. (2019). Design of a coordinated adaptive backstepping tracking control for nonlinear uncertain active suspension system. *Applied Mathematical Modelling*, 76, 479–494.

Tao, G. and Kokotovic, P.V. (1996). *Adaptive control of systems with actuator and sensor nonlinearities*. John Wiley & Sons, Inc.

Theunissen, J., Sorniotti, A., Gruber, P., Fallah, S., Ricco, M., Kvasnica, M., and Dhaens, M. (2019). Regionless explicit model predictive control of active suspension systems with preview. *IEEE Trans. on Industrial Electronics*, 67(6), 4877–4888.

Tyan, F., Hong, Y.F., Tu, S.H., Jeng, W.S., et al. (2009). Generation of random road profiles. *Journal of Advanced Engineering*, 4(2), 1373–1378.

Zarei, A., Mousavi, Y., Mosalanezhad, R., and Atazadegan, M.H. (2019). Robust voltage control in inverter-interfaced microgrids under plug-and-play functionalities. *IEEE Systems Journal*, 14(2), 2813–2824.

Zarei, A., Poutari, M.S., and Barakati, S.M. (2018). Trajectory tracking for two-degree of freedom helicopter system using a controller-disturbance observer integrated design. *ISA transactions*, 74, 99–110.